ISBN: 978-3-95450-231-8 ISSN: 2673-5490 doi: 10.18429/JACoW-IPAC2023-MOPL065

IMPACT OF DIPOLE QUADRUPOLAR ERRORS IN FCC-ee

C. García-Jaimes*, T. Pieloni, L. van Riesen-Haupt, M. Seidel, EPFL-LPAP, Lausanne, Switzerland
R. Tomás, CERN, Geneva, Switzerland

Abstract

FCC-ee performance is challenged by magnetic errors and imperfections. Magnetic design simulations predict a systematic quadrupolar component in the arc dipoles significantly impacting the machine optics. This paper studies the impact of this component in the beta-beating and explores potential mitigations.

INTRODUCTION

The simple way to schematically visualize the symmetrical design of the FCC-ee for the Z-mode [1] is as a circle with 16 main sections , including 4 interaction points (IPs), 4 intermediate straight sections (ISS) where the radiofrequency cavities (RF) are located and 8 intermediate arcs with FODO cells of 104.22 m in length each, see Fig. 1. The FODO cell structures are comprised of bending dipoles sandwiched between horizontally focusing and defocusing quadrupoles (QF and QD in the lattice), see Fig. 2. Note that alternative designs are currently being explored [2, 3].

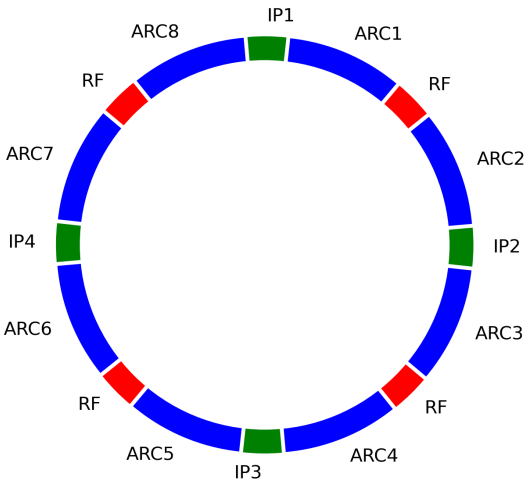

Figure 1: The IPs, ARCs, and RF are shown in green, blue, and red, respectively. It is noticeable that there is symmetry among the 4 IPs located diametrically opposite to each other for the lattice of Z-mode at energy of 45.6 GeV.

As in other particle accelerators, such as SuperKEKB [4], the existence of chromaticity around the IP mandates a local chromaticity correction scheme (LCCS) consisting of non-interleaved sextupole pairs, for the vertical plane is integrated on both IP sides, Fig. 3.

* cristobal.miguel.garcia.jaimes@cern.ch

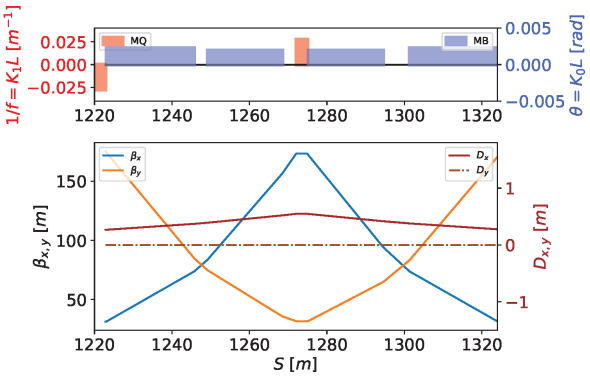

Figure 2: In this FODO cell for Z-mode at energy of 45.6 GeV, MQ and MB are the quadrupole and dipole magnets, respectively.

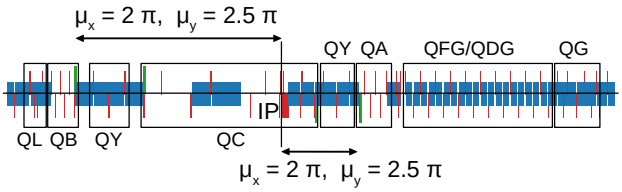

Figure 3: Terminology of quadrupoles in the FCC-ee experimental IPs. Dipoles, quadrupoles and sextupoles are shown, respectively, in blue, red and green [5].

In the FCC-ee, the periodic super-FODO structure consists of 5 FODO cells, each FODO cell has a phase advance ($\mu_{x,y}$) of $\frac{\pi}{2}/\frac{\pi}{2}$ [radians] for the horizontal and vertical planes. The phase advance is the fraction of a betatron oscillation between two points (usually a FODO cell) measured in radians. This scheme has been applied successfully at B-factories for more than 20 years [1]. To achieve sufficient dynamic apertures, a chromaticity correction with non-interleaved pairs of sextupoles could also be necessary [6]. The chromaticity is given by [7]:

$$\xi_{x,y} = \mp \frac{1}{4\pi} \oint \beta_{x,y}(k_1 - D_x k_2) ds \,, \qquad (1)$$

where D_x is the dispersion function, $\beta_{x,y}$ the β-function for each plane, k_1 and k_2 are the normalised quadrupole and sextupole strength respectively.

The values for the main optical functions can be found in Table 1. The four experimental IPs has the same optics design with a β^* of 100 and 0.8 mm for β_x and β_y, respectively at the Z-mode.

b_2 ERRORS IN FCC-ee

The FCC-ee magnet design team has anticipated a systematic quadrupolar error in the arc dipoles [9], known as

ISBN: 978-3-95450-231-8 ISSN: 2673-5490 doi: 10.18429/JACoW-IPAC2023-MOPL065

Table 1: Some parameters from the sequence-file for MAD-X [8] for the lattice of Z-mode at energy of 45.6 GeV [1].

Parameters for FCC-ee	
Length [m]	91174.117
Horizontal tune	214.260
Vertical tune	214.380
β_x^* [mm]	100
β_y^* [mm]	0.8
Horizontal Natural Chromaticity	-481.842
Vertical Natural Chromaticity	-3041.692
Horizontal Chromaticity	-1.165
Vertical Chromaticity	-1.911
Dispersion max [m]	0.624

b_2, which is dimensionless[1]. In this paper, the predicted magnetic quadrupolar errors have been incorporated into the dipoles in the arcs, and the resulting impact on various optical functions has been analyzed. The sign of the quadrupolar error depends on the arc in which the dipole is located because the beams cross in IPs and ISSs, moving from the inside to the outside ring or vice versa. This quadrupolar field causes a change in the β-function, D_x and $\mu_{x,y}$, which can be observed via the β-beating function and ΔD_x, $\mu_{x,y}$ -functions, defined as

$$\begin{aligned} \frac{\Delta\beta_{x,y}}{\beta_{x,y}} &= \frac{\beta_{x,y,\text{ error}} - \beta_{x,y,\text{baseline}}}{\beta_{x,y,\text{baseline}}}, \\ \Delta D_x &= D_{x,\text{error}} - D_{x,\text{baseline}}, \\ \Delta\mu_{x,y} &= \mu_{x,y,\text{ error}} - \mu_{x,y,\text{baseline}}, \end{aligned} \tag{2}$$

where $\beta_{x,y\text{ error}}$, $D_{x\text{ error}}$ and $\mu_{x,y\text{ error}}$ are the β-function, dispersion function and phase advance with the errors applied. $\beta_{x,y\text{ baseline}}$, $D_{x\text{ baseline}}$ and $\mu_{x,y\text{ baseline}}$ refer to the original lattice.

Due to the symmetry, the entire ring can be efficiently manipulated by working with only 25% of the lattice, as the families of quadrupoles are homogeneous in the arcs, IPs and ISSs. For example, the odd arcs (to the right of the interaction point) contain the same families of quadrupoles (QF4 and QD3) and even arcs (to the left of the interaction point) contain QF2 and QD1 in their FODO cells.

Taking into consideration the symmetry previously described for the FCC-ee, it is possible to model the expected magnetic quadrupolar errors in MAD-X. This allows for the calculation of the maximum error required to obtain a given β-beating. For example, in the case of 2% β_y-beating, the error b_2 in the dipoles should be 1.6×10^{-4} at a radius of 10 mm [10], as shown in Fig. 4.

To recover an appropriate behaviour in the IPs is mandatory to change the strength values (k_1) for the quadrupoles

[1] b_2 represents the normalized quadrupolar field error over the dipole field at a radius of 10 mm expressed in units of 10^{-4} [11].

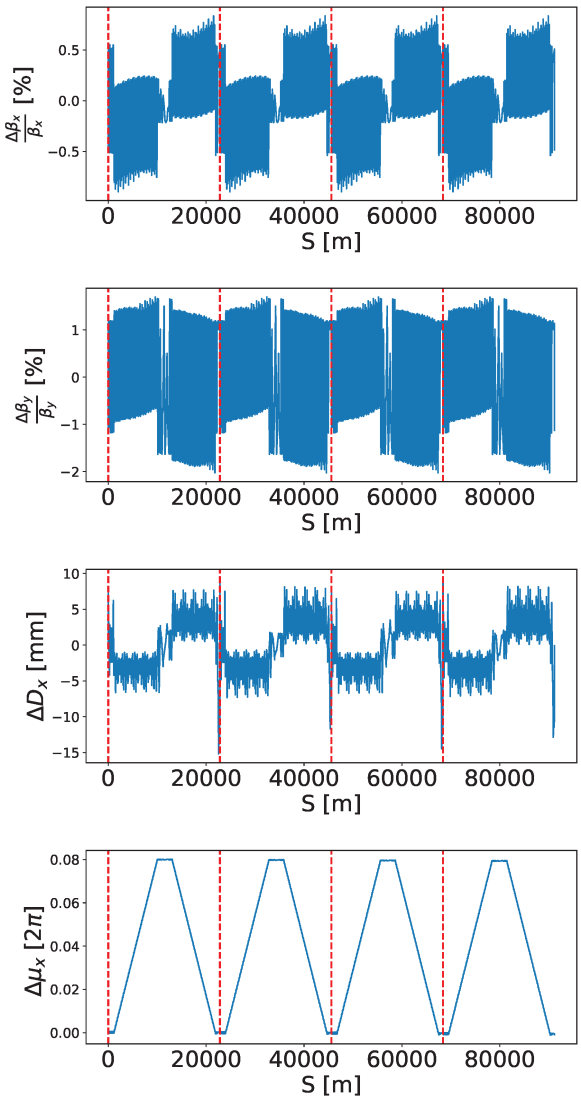

Figure 4: β-beating in percentage, ΔD_x in mm and $\Delta\mu_x$ in 2π along the collider length s due to quadrupolar errors in the dipole magnets of $b_2 = 1.6 \times 10^{-4}$ at a 10 mm radius. The red lines mark IPs.

QG, QH, QU, QRDR, QI, QL and QB, located both to the left and right of the IPs and the midpoint of the ISSs. Also the QF4, QF2 QD3 and QD1 in the arcs. The sextupoles strengths (k_2) were not changed. The nominal behaviour in the IPs can be achieved by working with the first IP, the first ISS, and the intermediate arcs between them, thanks to the existing symmetry already mentioned in the FCC-ee lattice for Z-mode. As a result, any changes made in this region will be replicated throughout the entire lattice. With this in consideration MAD-X matching can be used to recover: the correct phase advance in the arcs (and the horizontal and vertical betatron tune), Fig. 5, and the periodic behaviour in the IPs.

ISBN: 978-3-95450-231-8 ISSN: 2673-5490 doi: 10.18429/JACoW-IPAC2023-MOPL065

Table 2: Summary of optics parameters from MAD-X for FCC-ee Z-mode after matching. The Baseline lattice refers to the ideal lattice without errors. The second lattice includes b_2 errors, and the last one corresponds to the lattice after the application of matching.

Parameter	**Baseline Lattice**	**Lattice with b_2 errors**	**Lattice after the matching**
Horizontal tune	214.260	214.259	214.260
Vertical tune	214.380	214.379	214.380
Horizontal chromaticity	-1.165	-0.986	-0.916
Vertical chromaticity	-1.911	-3.461	-2.883
$\beta_{\mathrm{x,max}}$ [m]	4663.568	4684.116	4663.567
$\beta_{\mathrm{y,max}}$ [m]	9924.566	10037.678	9924.567
$D_{\mathrm{x,max}}$ [m]	0.624	0.632	0.787
Horizontal emittance ϵ_x [nm]	0.705	0.705	0.705
Damping partition numbers: J_x, J_y, J_z	0.999, 1.000, 2.000	0.999, 0.999, 2.000	0.999, 0.999, 2.000

The summary of the parameters obtained for the entire lattice after optics matching is presented in Table 2.

In the lattice with b_2 errors and matching the chromaticity changes by less than one unit; this is due to the changes of β-functions, quadrupole strengths, the quadrupolar errors in the dipoles and also the D_x at sextupoles. This is considerate like a small change since the vertical and horizontal natural chromaticity are -481.842 and -3041.692, respectively. This could be corrected with sextupoles.

Further analysis showed that β-beating is below 0.12% in the arcs but peaks occur in the ISSs (Fig. 5). This is not a problem as there are no IPs, RF cavities or sextupoles in the regions with larger β-beating.

As seen in Fig. 5, there is a change in the maximum dispersion due to the increase in the effective strength of the quadrupolar components by the errors in the dipoles. The largest change is observed in the ISSs, while in the FODO cells of the arcs, the change is around 0.05 m. The horizontal emittance (ϵ_x) is a measure of the spread of charged particles in the horizontal direction in a particle accelerator, the damping partition numbers (DPNs) are parameters that describe how quickly the longitudinal motion of a particle beam in a particle accelerator is damped. For both parameters there are not changes due to the application of b_2, see Table 2.

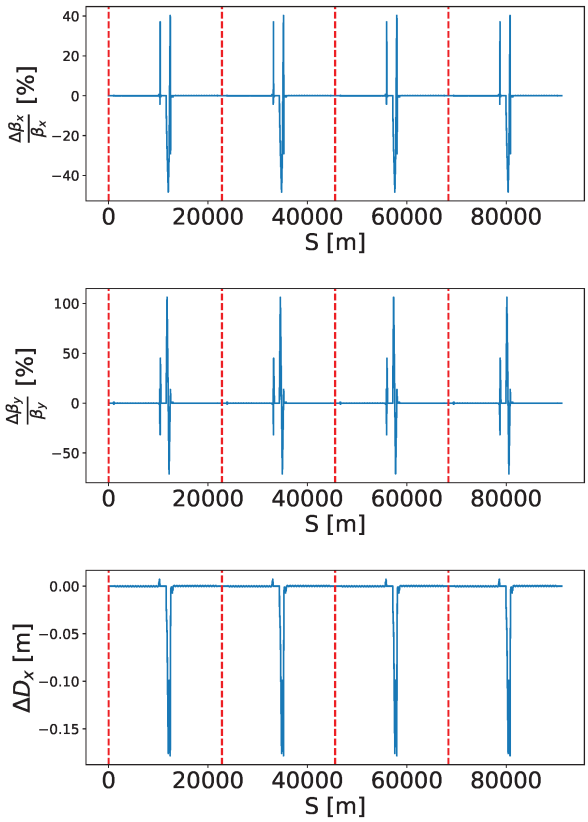

Figure 5: β-beating in percentage and ΔD_x in m along the collider length s after b_2 mitigation through matching.

CONCLUSIONS

We have shown that the systematic error b_2 predicted by the magnetic design can be absorbed by the optics design through changes in the k_1 of the quadrupoles in the ISS , the IPs and arcs. This achieved a β-beating of less than 0.12% and ΔD_x about 7.5 mm in the FODO cells and areas near the IPs after matching. Possible impact on the optics tuning performance remains to be studied [9, 10].

ACKNOWLEDGMENTS

We thank Katsunobu Oide and Jeremie Bauche for their insightful comments.

FCC-ee Beam Dynamics projects are supported by the Swiss Accelerator Research and Technology (CHART).

This project has received funding from the European Union's Horizon 2020 research and innovation programme under the Marie Skłodowska-Curie grant agreement No. 945363, EPFLglobaLeaders.

ISBN: 978-3-95450-231-8 ISSN: 2673-5490 doi: 10.18429/JACoW-IPAC2023-MOPL065

REFERENCES

[1] K. Oide *et al.*, "Design of beam optics for the future circular collider e+e- collider rings", *Phys. Rev. Accel. Beams*, vol. 19, p. 1111005, 2016.

[2] P. Raimondi, "Final Focus design with local compensation of geometric and chromatic aberrations", FCCIS 2022 Workshop, 5 Dec. 2022, https://indico.cern.ch/event/1203316/

[3] C. García-Jaimes, "Exploring FCC-ee optics design with combined function magnets", presented at Proc. IPAC'23, Venice, Italy, May 2023, paper MOPL066, this conference.

[4] Y. Ohnishi *et al.*, "Accelerator design at SuperKEKB", *Prog. Theoro. Exp. Phys.*, vol. 2013, no. 3, p. 03A011, 2013. doi:10.1093/ptep/pts083

[5] J. Keintzel *et al.*, " FCC-ee Lattice design", in *Proc. 65th ICFA Adv. Beam Dyn. Workshop High Luminosity Circular e+e- Colliders (eeFACT'22)*, Frascati, Italy, Sep. 2022, pp. 52–60. doi:10.18429/JACoW-eeFACT2022-TUYAT0102

[6] K. Oide and H. Koiso, "Dynamic aperture of electron storage rings with noninterleaved sextupoles". *Phys. Rev. E*, vol. 47, p. 2010, 1993. doi:10.1103/PhysRevE.47.2010

[7] A. Wolski and D. Newton, "Design of Electron Storage and Damping Rings", US Particle Accelerator School, https://uspas.fnal.gov/materials/13CSU/Lecture3.pdf

[8] MADX, http://madx.web.cern.ch/madx/

[9] T. K. Charles, B. Holzer, R. Tomas, K. Oide, L. van Riesen-Haupt and F. Zimmerman, "Alignment & stability challenges for FCC-ee", *EPJ Tech. Instrum.*, vol. 10, art. no. 8 (19 pages), 2023. doi:10.1140/epjti/s40485-023-00096-3

[10] R. Tomás *et al.*, "Progress of the FCC-ee optics tuning working group", presented at IPAC'23, Venice, Italy, May 2023, paper WEPL023, this conference.

[11] A. Milanese, "An introduction to Magnets for Accelerators", John Adams Institute Accelerator Course, https://indico.cern.ch/event/1101643/contributions/4635257/attachments/2372240/4058445